Rev.Adv.Mater.Sci. 5 (2003) 171-177

PROPERTIES OF YSZ AND CeGdO NANOPOWDERS PREPARED BY TARGET EVAPORATION WITH A PULSE-REPETITIVE CO_2-LASER

Yu.A. Kotov, V.V. Osipov, M.G. Ivanov, O.M. Samatov, V.V. Platonov, V.V. Lisenkov, A.M. Murzakayev, A.I. Medvedev, E.I. Azarkevich, A.K. Shtolz and O.R. Timoshenkova

Institute of Electrophysics, Ural Division of Russian Academy of Sciences, 106, Amundsena st., 620016 Ekaterinburg, Russia

Received: June 23, 2003

Abstract. The design and characteristics of a setup for producing oxide nanopowders are reported. Y_2O_3 – stabilized ZrO_2 (YSZ), Al_2O_3+YSZ and CeGdO nanopowders are prepared by target evaporation with a pulse-periodic CO_2-laser, followed by vapor condensation in air stream. Average laser radiation power is 600 W, pulse power ~ 10 kW. The output rates of YSZ and Al_2O_3+YSZ nanopowders are 15-20 g/h, and CeGdO nanopowder - 55-60 g/h. The grain mean size in the powders is 15nm. Data for the powder characteristics, as well as results of X-ray phase and structure analysis, are reported. The reasons of higher CeGdO output rate are discussed.

1. INTRODUCTION

Recent technologies of synthesizing bulk nanostructured materials with improved mechanical and novel electromagnetic and optical properties have generated interest in producing powders with nanometer-sized grains (nanoparticles). Nanoparticles can be produced by a variety of methods (for their detailed analysis, see, e.g. [1]). Laser radiation has not found wide recognition for this purpose because of a low output and high energy consumption of related techniques. At the same time, laser-assisted material evaporation and subsequent vapor condensation has been known for a long time. This approach to material production provides high-purity and fine-grain deposits, is cheap, and can be applied to various targets. However, its competitiveness with other approaches has been proved only recently [2].

We believe that the pulsed laser radiation mode must provide not only finer grains (because of an increased intensity and more efficient vapor removal from the hot zone) but also at least no higher energy consumption than in the CW mode. Our opinion relies on the fact that the probability of an elementary event of evaporation grows exponentially with the melt temperature and, hence, with the radiation peak power density [3]. Such a situation takes place up to optical breakdown. In [2], the pulsed mode was obtained by switching the *Q* factor of the laser cavity. *Q* switching imparts the specific shape to a laser pulse, because of which the advantages of the pulse-periodic mode of preparing nanodispersed powders cannot be revealed in the full measure. Moreover, *Q* switching decreases appreciably the laser efficiency. In this work, nanograin powders are produced with a pulse-periodic CO_2 laser excited by a pulse-periodic combined discharge [4].

This report deals with the production technology and characteristics of Y_2O_3 – stabilized ZrO_2 (YSZ), Al_2O_3+YSZ and CeGdO nanopowders prepared by

Corresponding author: M.G. Ivanov, e-mail: max@iep.uran.ru

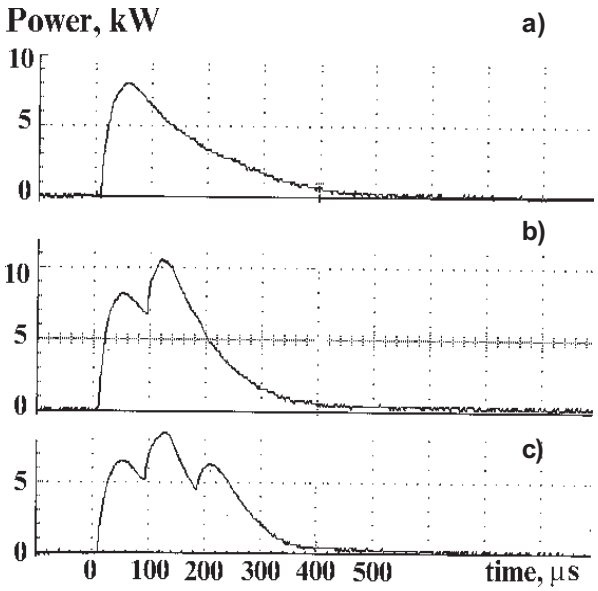

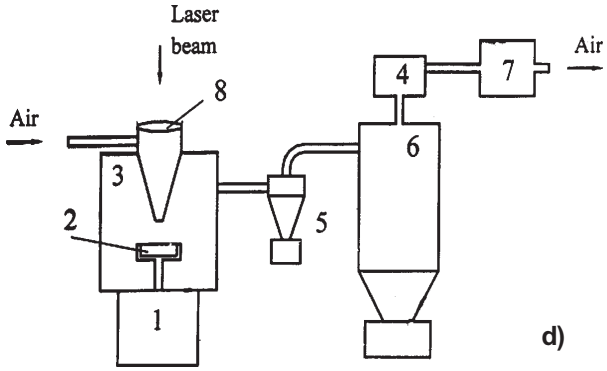

Fig. 1. (a-c) Waveforms of radiation pulses for different number of pulses in packet, (d) Experimental installation for nanopowder production.

evaporation of a target under irradiation from a pulsed CO_2 laser. Since the boiling point of CeO_2 and Gd_2O_3 is much lower than that of ZrO_2 and Y_2O_3, it was interesting to see how this factor influences the productivity and the particle size of the prepared powders.

2. EXPERIMENT

The nanopowders were prepared by target evaporation with the pulse-periodic CO_2-laser. The CO_2 laser excited by a pulse-periodic combined discharge has been described in detail in [4]. The laser has the following characteristics:

- Mean radiation power
  665-800 W
- Peak radiation power
  10-11.2 kW
- Diameter of the light beam in the outlet window 35 mm
- Radiation pulse length
  140-250 μs
- Pulse repetition frequency
  400-450 Hz
- Efficiency
  8.3-10%
- Power consumption
  8 kW

The typical waveforms of radiation pulses for different number of combined discharge pulses are shown in Figs. 1a-c. The laser radiation was focused on the target 2 through the lens 8 (Fig. 1d), which also served as the inlet window of the chamber 3. A special drive 1 rotated the target 2 and moved it linearly in the horizontal plane such that the laser beam traversed the target surface at a constant speed and the target evaporated uniformly. As the target was wearing out, it moved axially so that its surface remained in the plane of the focal spot. The focal distance of the KCl lens 8 was 10 cm. The focal spot was 0.45 mm in diameter. The scan rate of the beam over the target surface was 20 cm/s, which ensured displacement of the target for 0.043 cm during the pulse-to-pulse time. The fan 4 forced air through the evaporation chamber 3 and carried the powder to the cyclone 5 and the electric filter 6 where the powder was trapped. Air was cleaned additionally in the mechanical filter 7 and was returned by the fan to the chamber. The gas flow rate at the target surface was ~15 m/s.

The targets were prepared from a mixture of Y_2O_3 and ZrO_2, Al_2O_3+YSZ, CeO_2 and Gd_2O_3 powders so as to obtain powders whose composition would approach the optimal one. The initial powders had the specific surface S=2.8 m^2/g (as determined by the BET method on a GKh-1 chromatograph).

Both the raw materials and prepared powders were analyzed by X-ray techniques. The elemental composition was determined by spectral methods with a Jobin Yvon 48 instrument. Phase and structure analyses were performed with a DRON-4 X-ray diffractometer. The specific surface was found by the BET method using an argon-helium mixture with a GKh-1 chromatograph. The grain shape and grain

Table 1.

No	Raw material for target preparation	Powder after sedimentation
1	Powder mixture: ZrO_2, S = 20 m^2/g; 3.1Y_2O_3, S=4.5m^2/g	2.8YSZ: S = 68 m^2/g; *T: a* = 5.106 Å and *c* = 5.1638 Å, grain size *D* = 19 nm, weight of volatiles *m(V)* = 2.7wt% sediment 3.4YSZ: *T: a* = 5.1084 Å and *c* = 5.1674 Å; *D* = 26 nm; 6% of M/phase; Melted of target 5.2YSZ
2	Powder mixture: ZrO_2, S = 20 m^2/g, *T*= 45 and *M* = 55 wt%; 4.5Y_2O_3, S = 4.5 m^2/g	4.15YSZ:5 = 64.4m^2/g, *T*:a = 5.115 and *c* = 5.161 Å, *D* = 17 nm, *m(V)* = 2.6 wt%. Sediment 4.35YSZ; C-*a* = 5.13 e, *D* = 25 nm; 7% of *M* phase.
3	Powder mixture: ZrO_2, 5=51 m^2/g, *T* = 60 and *M* = 40 wt%; 9.1 Y_2O_3, S = 4.5 m^2/g	8.6YSZ: 5= 86 m^2/g; *C-a* = 5.1405 Å; *D* = 17 nm, *m(V)* = 2.4 wt% Sediment 8.9YSZ: *C-a* = 5.144 Σ, *D* = 25 nm. 7% of *M* phase
4	Powder 10.15YSZ, *S*= 6.1 m^2/g, C-a = 5.1448Å	9.85YSZ: 5= 79 m^2/g, *C-a* = 5.1459 Å, *D* = 18 nm, *m(V)* = 2.8 wt%. Sediment 10.4YSZ: C- *a* = 5.15 Å, *D* = 41 nm

Note: In raw material mixtures, the mole percentage of Y_2O_3 powder is indicated. *M, T,* and C stand for monoclinic, tetragonal, and cubic lattice, respectively.

size distribution were studied with JEM transmission and JSM-T220A scanning electron microscopes. The fractional composition of the powders was investigated by sedimentation analysis. The content of moisture and volatiles was determined thermogravimetrically with a Q1500 instrument.

3. RESULTS AND DISCUSSION

For YSZ and Al_2O_3+YSZ, the output rate was 15-20 g/h, for CeGdO ~ 60 g/hour. The analyses of the powders showed that they are weakly agglomerated and have two fractions with greatly differing sizes. The first fraction (Fig. 2a) consists of spherical grains with sizes from 0.2 to 2.0 mm and accounts for 3-7 wt%. Presumably, it forms by splashing the liquid phase, since the composition of these grains either is close to that of the raw material or is enriched by the component with a higher point of evaporation, while the other fraction (nanofraction) always has a deficiency of this component compared with the raw material (Table 1). The coarser fraction sometimes contains shapeless grains of size to 10 μm (possibly, target fragments). From the grain size distribution (Fig. 2c) in the fraction remaining in the suspension (Fig. 2b), it follows that 98% of grains have sizes < 40 nm and only 0.25% of grains have a size from 65 to 100 nm. The latter grains are nearly spherical and slightly faceted.

Upon sedimentation, the grain specific surface usually decreases by 10%, which indicates that the powders are slightly agglomerated. However, after the sedimentation, the powders have a one order of magnitude higher bulk weight, becoming more producible for subsequent applications.

The study of the phase composition and structure of the YSZ powders (Table 1) showed that they are single-phase and their averaged lattice parameter is well described by a straight line (Fig. 2d) whose initial portion coincides with data for pure ZrO_2 [5] obtained by the plasma-chemical method and containing 90% of the tetragonal phase. Our data for ZrO_2 nanopowders obtained by electrical explosion and containing from 55 to 65 wt% of the tetragonal phase [6] fall into the range shown in Fig. 2d.

The study of the elemental composition of the powder mixtures (Table 2) suggests that a decrease in the high-temperature component content in these samples, prepared by co-evaporation, is much more significant than in the YSZ powders. This decrease becomes more evident as the content of the low-temperature component (Al_2O_3, point of evaporation T = 3800K, the melting point T_m = 2320K) grows.

Table 2.

Target composition	*Target material*	*Powder after sedimentation*
Powder mixture *A*40+1.65YSZ60	Al_2O_3 : *S* = 74 m^2/g; γ = 20 wt%; δ = 80 wt% 1.65 YSZ: *S* = 7.76 m^2/g. *M*=58 and *T*=42wt%. Grain size *D* = *70* nm.	*A*41.1+1.45YSZ58.9, *S*=80.6 m^2/g, *m(V)* = 4.9 wt% Composition and structure: 1.45YSZ: *T*-31 wt%: *a* = 5.095 and *c* = 5.156 Å, *D* = 11 nm. *K* - 28 wt%: a = 4.924 Å, *D* = 6 nm. γ = Al_2O_3-20wt%, *D*= 10nm. Amorphous Al_2O_3 - 21wt%
Powder mixture *A*85+M.635YSZ15	___ " ___	*A*88.8+1.15YSZ 11.2, *S*= 86 m^2/g, *m(V)* = 4.8 wt%. Preliminary composition and structure: cubic and tetragonal 1.15YSZ and γ-Al_2O_3, amorphous Al_2O_3; diffraction 2 pattern interpretation is being continued

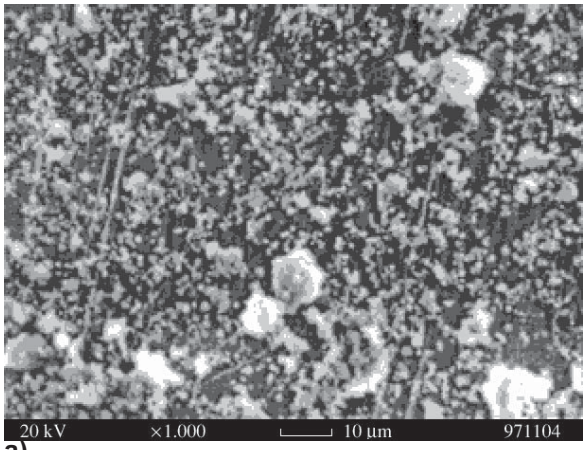

a)

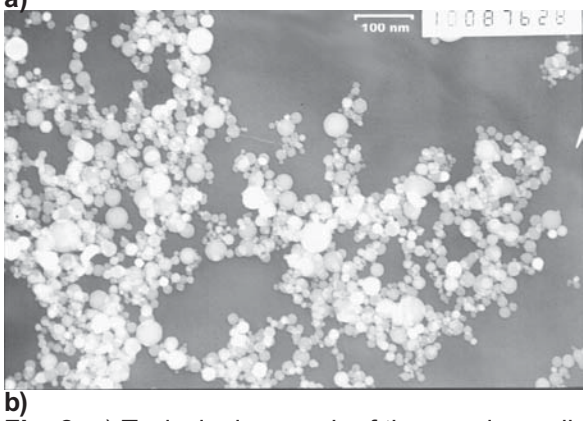

b)

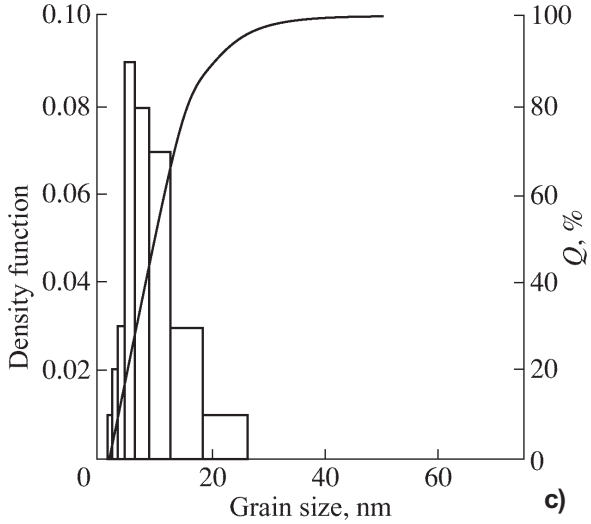

c)

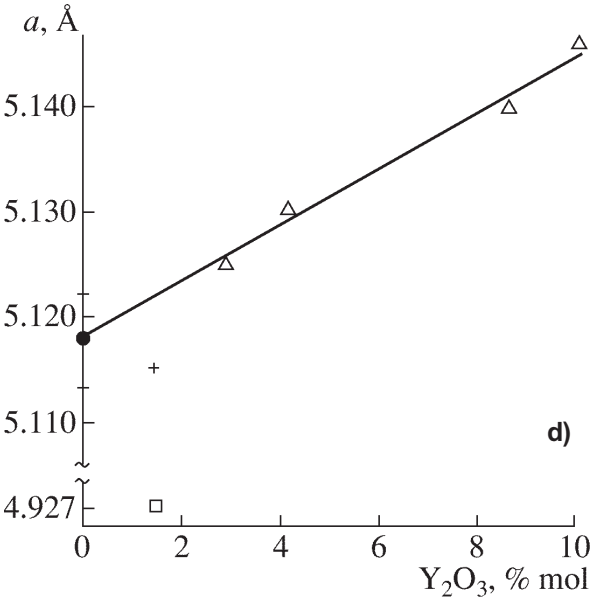

d)

Fig. 2. a) Typical micrograph of the powder sediment. b) Typical micrograph of the powder fraction from the suspension. c) Grain size distribution. d) YSZ lattice parameter vs. Y_2O_3 content: (Δ) our data for the YSZ powder, (●) published data for ZrO_2 with 90 wt% of the tetragonal phase, (+) tetragonal phase of the *A*40+1.45 YSZ mixture, and ( ) cubic phase of the *A*40+1.45 YSZ mixture.

For example, in mixture 1, the YSZ content decreased by =2% and the Y_2O_3 content in YSZ, by 12%. In mixture 2, the associated values are 25 and 30%, respectively. In other words, the initial equality of the component volumes (mixture 1) and weights (mixture 2) in the targets is violated in the powders.

The phase composition of the powders also turned out to be unusual. For example, in mixture 1, about 40 wt% of 1.45YSZ is in the cubic phase. Moreover, the lattice parameter of both the cubic and the tetragonal phases is much smaller than could be expected from the concentration dependence (Fig. 2d). The monoclinic phase is absent at all. It can be proposed that in the liquid state, some amount of Al_2O_3 dissolves in YSZ, forming the solid solution. Assuming that the YSZ lattice parameter varies linearly from the value 5.123 Å for pure 1.45YSZ according to the zirconium-to-aluminum atomic radius ratio, 1.2, one can estimate the amount of Al_2O_3 dissolved in the YSZ lattice. These estimates show that the tetragonal phase occupies =0.7 wt% and the cubic phase, = 19.4 wt%. From the diffraction patterns, it also follows that Al_2O_3 is partially in the amorphous state. If it is assumed that 1.45YSZ is entirely crystalline, the amount of the amorphous Al_2O_3 in the power considered is =21 wt%.

The diffraction pattern for the 488.8+1.15YSZ11.1 powder was still harder to interpret, because the line asymmetry and the background level were very high. It is only clear that an increase in the Al_2O_3 content does not increase the fraction of the cubic modification relative to the tetragonal one in the powder after laser synthesis. However, upon sedimentation, a significant fraction of the powder in the tetragonal phase precipitates. The high asymmetry of the diffraction lines, especially for the tetragonal phase, raises an error in determining the weight composition of the phases and grain size. This and also the fact that the YSZ tetragonal phase, having a grain size of 6 nm, almost completely precipitated lead us to suggest that YSZ tetragonal grains are covered by aluminum oxide and seem to have a greater size. That is why they precipitate upon sedimentation. Thus, the above data lead us to conclude that the powders prepared in this work are of interest for further investigating their structure, which depends on the Al_2O_3/YSZ ratio in the starting mixture.

We prepared 780 g of CeGdO powder having the specific surface S=57±4 m^2/g. The sedimentation analysis in isopropyl alcohol demonstrated that the powder contained ~8 wt % particles larger than 200 nm in size (Fig.3b). They represented a mixture of spherical particles up to 1.5 μm in diameter, which probably resulted from spattering of the liquid bath on the target, and shapeless particles up to 5 μm in size, which probably comprised fragments of the target. After sedimentation S was 56±4 m^2/g, i.e. changed little, because precipitation of coarse particles was accompanied by small agglomeration of the powder.

The transmission electron microscopic examination (JEM-200) showed that the particle shape varied between cubic and spherical (Fig. 3c). The constructed particle size distribution (1583 particles, Fig. 3d) proved to be close to the normal logarithmic distribution with the geometric mean diameter d_g = 9.4 nm and the deviation from this diameter equal to σ_g = 1.7. At > 40 nm only one particle with d = 50, 60, 65, 80, and 195 nm was found, i.e. over 99% particles had d < 40 nm, as was in YSZ powders.

The XRD showed that the powder had one phase and comprised Gd solid solution in the cubic lattice of CeO_2 with the lattice constant of 0.5424 nm and the grain size D = 19 nm (Scherer's method). Since coarse particles contributed most to the grain size and $D > d_g$, one might infer that the powder particles were monocrystalline.

The spectral analysis (Jobin Yvon 48 spectrometer) demonstrated that the nanopowder approached the wanted composition. In terms of CeO_2 and Gd_2O_3 and taking into account 2.8 mass % volatiles, which were determined from the TGA analysis, the mass concentration of oxides in the powder was 0.782 and 0.218 respectively.

As was noted in the foregoing, the productivity was 60 g/hour, i.e. 3 times larger than the YSZ output rate. This was due partly to the fact that the shape of the radiation power pulse was improved a little: it was shorter; the maximum power increased by 10%; and the pulse repetition frequency was raised from 400 to 435 Hz. However, the main factor probably was a considerable reduction in the energy required for evaporation of the mixture. The calculation, which was made using thermodynamic data for ZrO_2, Y_2O_3, CeO_2 and Gd_2O_3 oxides [7, 8], showed that the energy needed for heating and evaporation of the $0.83ZrO_2$+$0.17Y_2O_3$ mixture (corresponding to 10YSZ) and the test $0.654CeO_2$ + $0.346Gd_2O_3$ mixture under adiabatic conditions was $W \approx$ 7.9 kJ/g and 4.7 kJ/g respectively. Since the pulse energy did not change (~1.5 J) and the energy W decreased ~1.7 times, one might expect

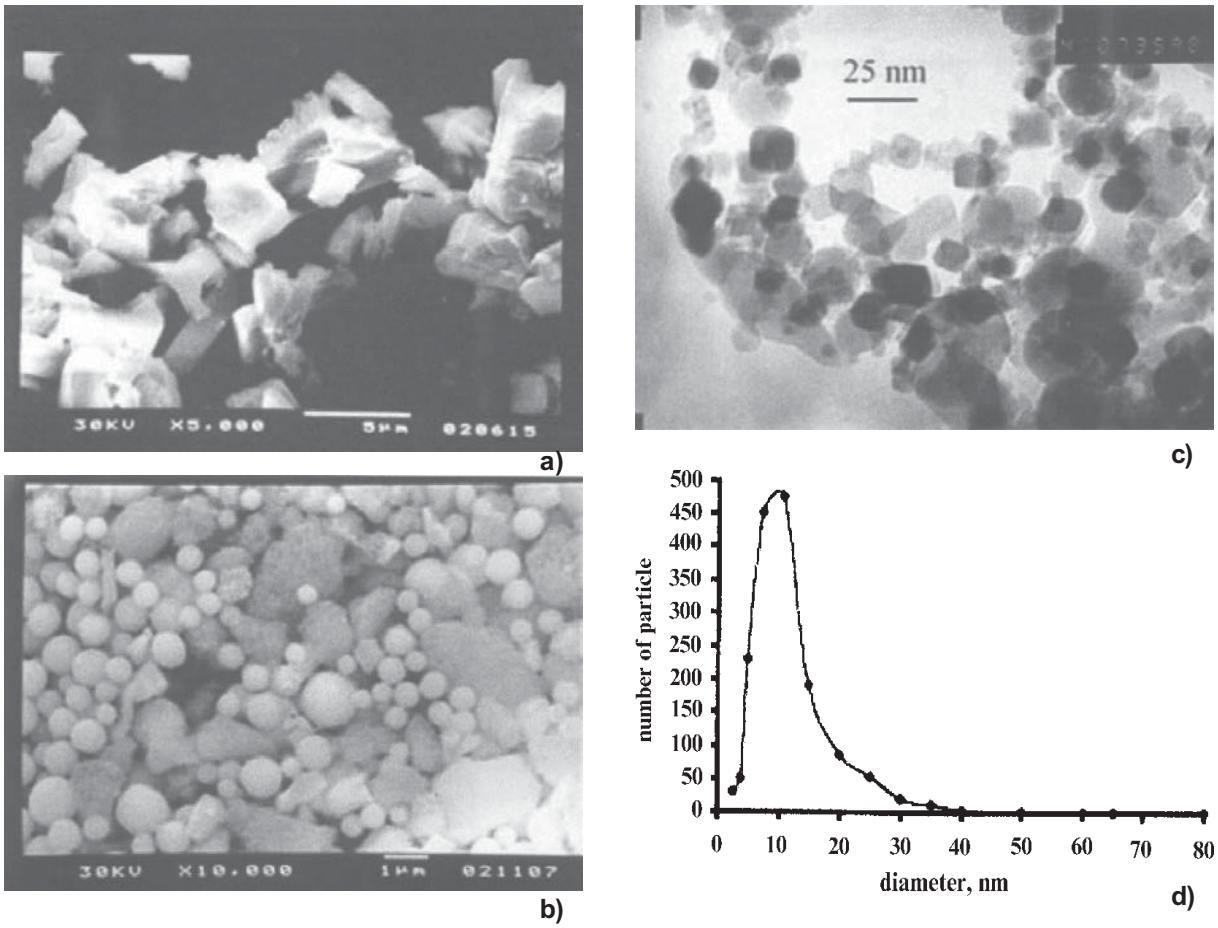

Fig. 3. Photographs of particles: a – initial powders of CeO_2; b – particles from the sediment of suspension; c – particles from the suspension; d - particle size distribution in the $Ce_{0.78}Gd_{0.22}O_{2-d}$ powder after sedimentation.

the corresponding increase in the productivity. Moreover, since the radiation pulse was not rectangular and the sublimation energy of the test mixture was smaller, the power density, which was sufficient for evaporation, could be maintained for a longer time, also leading to the increase in the productivity.

The fact that the increase in the productivity was not followed by growth of the particles as compared to 10YSZ had two explanations. Firstly, the calculation showed that the number of molecules only increased ~1.9 times when the mass of the test mixture was 3 times as large as the mass of 10YSZ. Secondly, the energy was injected to the target in pulses (the mean pulse power of > 8 kW at the power density of $5.2 \cdot 10^6$ W/cm^2). As a result, the target was overheated considerably. The vapor was ionized partially and scattered to the ambient gas at a speed of several km/s. The vapor concentration dropped quickly, while the vapor cooling was delayed, because the radiation pulse continued heating the vapor during the initial stage of scatter. Into our installation chamber (Fig. 1d), the vapor moved towards radiation. Moreover, the power energy was ~10 times larger than the one required for the mass evaporated per pulse ($3.8 \cdot 10^{-5}$ g). Part of this excess energy obviously was consumed for heating of the expanding cloud of the ionized vapor. Under these conditions, before the vapor could condense, its concentration dropped to a level when the particles did not grow over ~10 nm in size as a result of condensation and possible subsequent coalescence. This made one think that the evaporation productivity could be increased further. However, efforts in this direction (expansion of the evaporation surface area) were a failure. Probably, causes responsible for the energy loss need be determined

more carefully (radiation from the torch area, thermal conductivity of the target, melting of its surface layer, losses in the plasma, the scatter energy loss, etc.). These issues have been beyond the scope of the present study and will be covered in future.

4. CONCLUSION

It was found that evaporation of targets using the pulse-periodic CO_2 laser represents an efficient method for production of weakly agglomerated nanopowders of complex compounds with particles having the characteristic size of ~10 nm and a narrow size distribution. An analysis of the obtained results showed that the main factor, which determines the productivity of the installation having certain characteristics, is the specific energy required for evaporation of the material.

ACKNOWLEDGEMENT

This study was supported by the ISTC (Project No. 2277p).

REFERENCES

[1] A. I. Gusev and A. A. Rempel, *Nanocrystalline Materials* (Nauka, Ekaterinburg, 2000).
[2] E. Muller, Ch. Oestreich, U. Popp *et al.* // *Kona* (Hirakata, Jpn.) **13** (1995) 79.
[3] S. I. Anisimov, Ya. A. Imis, G. S. Romanov and Yu. V. Khodyko, *High Power Radiation Effect on Metals* (Nauka, Moscow, 1970).
[4] V.V.Osipov, M.G.Ivanov, V.V.Lisenkov and V.V.Platonov // *Quantum Electronics* **32** (2002) 253.
[5] V. N. Troitskii, E. N. Kurkin, V. I. Torbov *et al.* // *Neorg. Mater.* **30** (1994) 1436.
[6] Y. A. Kotov, I. V. Beketov, A. M. Murzakaev *et al.*// *Mater. Sci. Forum* (1996) 913.
[7] E.K. Kazenas and D.M. Chizhikov, *Pressure and Composition of Vapor over Oxides of Chemical Elements* (Nauka, Moscow,1976), in Russian.
[8] P.A. Arseniev, L.M. Kovba, Kh.S. Bagdasarov, *et al*., *Compounds of Rare-Earth Elements. Systems with Oxides of 1- to 3-Group Elements* (Nauka, Moscow,1983).